ORIGINAL ARTICLE

Protective role of Hsian-tsao ethanol extract against body fat, serum lipid profiles, and hepatic lipid profiles in high-fat diet-fed rats

Ching-Chang Cho [a,1], Gow-Chin Yen [b,1], Hsin-Yi Lee [a], Chun-Tse Tsai [a], Wei-Tang Chang [c], Chin-Lin Hsu [a,d,*]

[a] Department of Nutrition, Chung Shan Medical University, Taichung, Taiwan
[b] Department of Food Science and Biotechnology, National Chung Hsing University, Taichung, Taiwan
[c] Department of Nutrition and Health Sciences, Chinese Culture University, Taipei, Taiwan
[d] Department of Nutrition, Chung Shan Medical University Hospital, Taichung, Taiwan

Abstract

This study investigated the preventive effects of a 40% ethanol extract of Hsian-tsao (40EEHT) on obesity in high-fat diet (HFD)-induced obese rats. Male Wistar rats were administered 0, 100, 200, or 500 mg/kg of 40EEHT, resulting in reduced body weight, total body fat, and hepatic tissue weight after 8 weeks. 40EEHT also decreased adipocyte size, improved lipid profiles, alleviated oxidative stress, and enhanced hepatic antioxidant enzyme activities. Additionally, it regulated fatty acid metabolism by reducing lipogenesis and increasing lipolysis and β-oxidation, suggesting its potential as an anti-obesity dietary supplement.

Keywords: Anti-Obesity, Ethanol extract of Hisan-tsao, High-fat diet, *Mesona procumbens* Hemsl., Oxidative stress

1. Introduction

Recently, obesity has been recognized as a chronic positive energy balance due to insufficient physical activity and excessive dietary intake, leading to an impaired ability to store body fat effectively [1]. The incidence of obesity continues to rise worldwide, making it an increasingly critical public health concern. Obesity is associated with disorders such as fatty liver disease, dyslipidemia, hypertension, cancer, and type II diabetes, all of which contribute significantly to increased rates of disability and mortality [2]. Excessive dietary fat and reduced energy expenditure lead to fatty acid synthesis in adipose and hepatic tissues [3,4], which may further promote the development of metabolic syndrome [5,6].

Dietary supplements, including bioactive ingredients and crude extracts derived from plants, are commonly used to prevent and manage obesity [7–9]. In folk medicine, Hsian-tsao (*Mesona procumbens* Hemsl.) has demonstrated potential in ameliorating conditions such as heat shock, liver injury, and metabolic syndrome [10–13]. Hsian-tsao exhibits a diversity of beneficial activities, including hypolipidemic, hypotensive, and hypoglycemic effects, as well as antibacterial, antioxidant, anti-inflammatory, and anti-mutagenic properties [14–18]. In recent studies, derivative compounds from the methanol extract of Hsian-tsao have shown anti-adipogenic effects by inhibiting fatty acid anabolism in 3T3-L1 adipose cells [19]. Additionally, in RAW 264.7 cells, the crude polysaccharide and ethanol extract of Hsian-tsao have exhibited strong inhibitory effects on reactive oxygen species generation and methylglyoxal-mediated glycation, and have reversed cytokine levels related to wound healing in 3T3-L1 cells [20].

Oxidative stress is a metabolic by-product that can significantly influence the progression of metabolic

Received 20 May 2024; accepted 27 August 2024.
Available online 31 March 2025

* Corresponding author at: Department of Nutrition, Chung Shan Medical University, Taichung, Taiwan.
E-mail address: clhsu@csmu.edu.tw (C.-L. Hsu).
[1] These authors contributed equally to this work.

https://doi.org/10.38212/2224-6614.3527

syndrome [21,22]. Phenolic acids exhibit high antioxidant activity, which can notably ameliorate the pathophysiology of obesity [23,24]. Moreover, abundant phenolic acids, such as *p*-coumaric acid, protocatechuic acid, vanillic acid, caffeic acid, chlorogenic acid, and *p*-salicylic acid, have been identified in Hsian-tsao [14,25]. Xu et al. (2020) demonstrated that the intervention of 50 mg/kg/day caffeic acid for 30 days significantly reversed body weight, lipid accumulation, and gut microbiota alterations in HFD-fed rats [26]. Phenolic acids in Mageu significantly reduced lipid droplet accumulation and enhanced antioxidant capacity in 3T3-L1 cells [27]. Additionally, caffeic acid, chlorogenic acid, apigenin, and naringenin found in the methanol extract of *Caralluma edulis* exhibit strong antioxidant, anti-obesity, anti-atherosclerotic, and antihypertensive effects in obese Wistar albino rats [28].

According to our preliminary study, 40EEHT exhibited the highest total polyphenol, total phenolic acid, and TEAC levels in 3T3 adipocytes. Subsequently, an *in vivo* investigation was conducted using 40EEHT. This report aims to explore the anti-obesity activities of the ethanol extract of Hsian-tsao in obese rats. Additionally, we will confirm whether the beneficial effects of the ethanol extract of Hsian-tsao are due to its regulation of molecular mechanisms involved in fatty acid synthesis, lipolysis, fatty acid transport and storage, or β-oxidation.

2. Methods

2.1. Preparation of ethanol extracts of Hsian-tsao

Hsian-tsao (Taoyuan No. 1) was provided from the farmers' association of Guanxi Town (Hsinchu, Taiwan). 5 g Hsian-tsao dry powder was supplemented with 40% ethanol solutions at room temperature for 24 h. The extract of Hsian-tsao was concentrated and lyophilized for further use. The weight of 40EEHT is 0.923 g, and the extraction yield of 40EEHT is 18.25 ± 1.44%. The extraction yields (%) = (weights of 40EEHT/weights of Hsian-tsao powder) × 100%.

2.2. Experimental animal design

In this study, five-week-old male Wistar rats (BioLASCO Taiwan Corp., Ltd in Yilan, Taiwan) were individually held in cages within the animal facility at Chung Shan Medical University, under controlled environments of humidity (55 ± 5%), temperature (25 ± 1 °C), and a 12:12 h light–dark cycle for seven days. The procedures employed in all animal experiments were executed in accordance with the guidelines established through the National Institutes of Health (NIH). The investigation was accepted by the Institutional Ethics Committee of Chung Shan Medical University in Taichung, Taiwan, and the IACUC protocol number is 1619. High-fat diet (32% fat, w/w) was prepared from AIN-93G diet (Hansen Trading Co., Ltd., New Taipei City, Taiwan) with 7% soybean oil and 25% lard. Six-week-old rats were distributed into five groups (n = 10): normal diet (ND), high-fat diet (HFD), HFD + 100 mg/kg of 40EEHT, HFD + 200 mg/kg of 40EEHT, and HFD + 500 mg/kg of 40EEHT, respectively. We recorded body weight, water intake, and feed intake once a day. Rats were sacrificed with CO_2 inhalation in an overnight fasting condition after 8 weeks of intervention, and the final body weight was measured, then we calculated body weight change and the feeding efficiency. Blood was collected from the abdominal aorta of rats, and then serum was obtained after centrifugation. Organs (kidney, spleen, liver, lung, and heart) and tissue (mesenteric adipose, inguinal adipose, retroperitoneal adipose, epididymal adipose, perirenal adipose) were directly removed and weighed, and then they were treated using liquid nitrogen.

2.3. Determination of serum parameters of rats

The contents of low-density lipoprotein-cholesterol (LDL-C) (Cat No. 141319910930), total cholesterol (TG) (Cat No. 157109910917), triglycerides (TC) (Cat No. 113009910917), creatinine (Cat No. 11711 9910917), uric acid (Cat No. 130219910704), aspartate aminotransferase (AST) (Cat No. 126019910917), alanine aminotransferase (ALT) (Cat No. 12701 9910917), sodium (Cat No. 148089910921), chloride (Cat No. 112219910921), calcium (Cat No. 11181 9910917), phosphate (Cat No. 152119910930), and potassium (Cat No. 152219910921) in serum were detected by commercial kits (Diasys Co Ltd., Holzheim, Germany). The levels of serum glucose were detected with a glucose assay kit (Cat No. GL8038, Teco Diagnostics, Randox Laboratories Co Ltd., Antrim, UK). The ketone body contents were estimated by a standard commercial ketone body kit (Cat No. ab272541, Abcam, Cambridge, UK).

2.4. Histological analysis of hepatic and adipose tissues of rats

The tissue samples of rats were fixed overnight in a 10% buffered formaldehyde solution at a pH of 7.4, then sectioned at 5 μm. The tissue samples were

conducted using a Hematoxylin and eosin (H&E) staining protocol [29].

2.5. Determination of hepatic and fecal lipid profiles of rats

We extracted the lipids in liver and feces as the method of Tzang et al. (2009) [30], and total triglyceride was estimated using a Triglyceride-GPO liquid reagent set (TG reagent) (Cat No. T531-150, Teco Diagnostics, Anaheim, CA, USA), and cholesterol was measured using a cholesterol kit (Cat No. CH200, Teco Diagnostics, Randox Laboratories Co Ltd., Antrim, UK).

2.6. Determination of serum and hepatic antioxidant capacities of rats

Analysis of the antioxidant capacity was performed by the Trolox equivalent antioxidant capacity (TEAC) assay that was conducted by Arts et al. (2004) [31]. ABTS free radical cations were produced using the mixing of peroxidase (4.4 U/mL), H_2O_2 (50 μmol/L), and ABTS (100 μmol/L). 0.25 mL a mixture of ABTS, H_2O_2, and peroxidase was added to 0.25 mL of serum and combined with 1.5 mL ddH_2O. OD_{734} was used to measure the sample solution after mixing for 10 min. The TEAC value (μmol/mL) was examined from the reduction in the optical density values at 734 nm following the addition of the reactant.

2.7. Determination of serum and hepatic malondialdehyde (MDA) of rats

Determination of MDA was conducted according to the methods of Bird and Draper (1984) [32]. To determine MDA levels, 2.5 mL sample solution was collected from rats well mixed with 5 mL 10% trichloroacetic acid (TCA) reagent. Supernatant was collected from the mixture solution after centrifuged at 12,000×*g* for 10 min under 4 °C. Supernatant interacted with 0.67% TBA-HCL solution (1:1), incubated for 10 min at 95 °C. MDA levels (nmol/mL) was determined through A 1,1,3,3-tetramethoxypropane-derived standard curve.

2.8. Determination of hepatic GSSG and GSH of rats

Liver tissue was suspended in a PBS buffer (pH 7.0), centrifuged at 12,000×*g* for 10 min to separate the components. We collected the supernatant for further used. Quantitation of GSSG and GSH were estimated using a glutathione assay kit (Cat No. 703002, Cayman Chemicals, USA). GSH and GSSG levels (nmol/mg) were estimated at OD_{405}.

2.9. Determination of serum and hepatic antioxidant enzymes of rats

GSH peroxidase (GPx) activity was performed as described in Lawerence and Burk (1976) [33]. A 20 μL hepatic homogenate solution was combined with 180 μL 100 mM PBS buffer at a pH of 7.0, which contained 1 U/mL GRd, 1 mM GSH, 0.2 mM NADPH, 1 mM EDTA-2Na, and 1 mM NaN_3 at around 25 °C for 2 min. The absorbance alteration at OD_{340} was detected for 1 min. The GPx activity was quantified via the extinction coefficient of NADH (6220 $M^{-1}cm^{-1}$) and, with the resulting value expressed in (unit/min/mg). GSH reductase (GRd) activity was quantified via Bellomo et al. (1987) [34]. A 20 μL hepatic homogenate solution was combined with 180 μL 100 mM PBS buffer at a pH of 7.0 with 0.1 mM NADPH, 1 mM $MgCl_2 \cdot 6H_2O$, and 5 mM GSSG at around 25 °C for 2 min. The absorbance alteration at OD_{340} was detected for 1 min. The extinction coefficient of NADH was used to quantify the GRd activity, and the resulting value expressed in (unit/min/mg). The activity of catalase was detected via the method of Shangari and O'Brien (2006) [35]. 100 μL hepatic homogenate solution combined with 900 μL of PBS buffer at a pH of 7.0, containing 25 mM H_2O_2. The absorbance alteration at OD_{340} was measured for 1 min. The catalase activity (unit/min/mg) was measured with the extinction coefficient of H_2O_2 (39.5 $M^{-1}cm^{-1}$).

2.10. Determination of fatty acid metabolism regulation of rats

The E.Z.N.A™ tissue RNA kit (Cat No. D5625-01, Omega Bio-Tek, USA) was used to isolate total RNA from the perirenal adipose tissue. The SYBR® Green RT-PCR reagents kit was used to conduct quantitative real-time PCR (Applied Biosystems, USA). Relative gene level was executed via the method in Livak and Schmittge (2001) [36]. Cycling procedures were 15 min at 95 °C, followed by 94 °C for 15 s, 51 °C for 30 s, and 72 °C for 30 s (40 cycles). The primer pairs of genes in perirenal adipose tissues were used (forward and reverse, respectively): *ACC*, 5′-gaatctcctggtgacaatgcttatt-3′ and 5′-ggtcttg ctgagttgggttagct-3′; *ACO*, 5′-catggccaagcccaacat-3′ and 5′-cgcccagtttgaaggaaatc-3′; *Adiponectin*, 5′-catgg ccaagcccaacat-3′ and 5′-cgcccagtttgaaggaaatc-3′; *AMPK*, 5′-acacctcagcgctcctgttc-3′ and 5′-ctgtgctg gaatcgacact-3′; *aP2*, 5′-cctttgtggggacctggaaa-3′ and 5′-tgaccggatgacgaccaagt-3′; *ATGL*, 5′-tgtggcctcat

tcctcctac-3′ and 5′-agccctgtttgcacatctct-3′; *β-actin*, 5′-tacaatgagctgcgtgtgg-3′ and 5′-tggtggtgaagctgtagcc-3′; *CD36*, 5′-gatgacgtggcaaagaacag-3′ and 5′-tcctcgg ggtcctgagttat-3′; *CPT-1*, 5′-gctcgcacattacaaggacat-3′ and 5′-tggacaccacatagaggcag-3′; *FAS*, 5′-cttgggtgc cgattacaacc-3′ and 5′-gccctcccgtacactcactc-3′; *FATP1*, 5′-gtgcgacagattggcgagtt-3′ and 5′-gcgtgaggatacggct gttg-3′; *HSL*, 5′-cccataagaccccattgcctg-3′ and 5′-ctgcc tcagacacactcctg-3′; *LPL*, 5′-cccagctttgtcatcgagaag-3′ and 5′-cctggcacagaagatgaccttt-3′; *PGC-1α*, 5′-caatgag cccgcgaacatat-3′ and 5′-caatccgtcttcatccaccg-3′; *PGC-1β*, 5′-ttgacagtggagctttgtgg-3′ and 5′-gggcttatatgg aggtgtgg -3′; *PPAR-α*, 5′-catcgagtgtcgaatatgtgg-3′ and 5′-gcagtactggcatttgttcc-3′; *PPAR-γ*, 5′- catgaccag ggagttcctcaa-3′ and 5′- agcaaactcaaacttaggctccat -3′; *SCD-1*, 5′-ctgacctgaaagctgagaag-3′ and 5′-acaggctg tgcaggaaagtt-3′; *SIRT1*, 5′-gatctcccagatcctcaagcc-3′ and 5′-caccgaggaactacctgat-3′; *SREBP-1c*, 5′-agccatgg attgcacatttg-3′ and 5′-ggtacatctttacagcagtg-3′; *TNF-α*, 5′-ggctccctctcatcagttcca-3′ and 5′-gcttggtggtttgctac ga-3′; *UCP-1*, 5′-acactgtggaaagggacgac-3′ and 5′-catc tgccagtatgtggtgg-3′.

2.11. Statistical analysis of the results

Reported values are revealed as means ± SEM, and the statistical analyses of the results were conducted via the version 13.0 of statistical product and service solutions (SPSS) (SPSS Inc. in Chicago, IL, USA). All data were analyzed via PROC ANOVA analysis. Duncan's multiple-range test was used to determine the differences between groups, with a *p*-value below 0.05 defined as statistically significant.

3. Results

3.1. Effect of 40EEHT on growth parameters in HFD-fed rats

In Table 1, the study found that the initial body weights showed no significant differences among the groups. However, weight change and final body weight were significantly increased after HFD feeding, but these increases were markedly reversed in the HFD + 200 mg/kg and 500 mg/kg 40EEHT groups. Feed intake was similar between the ND and HFD groups but was markedly reduced in the HFD + 500 mg/kg 40EEHT group. HFD feeding significantly enhanced feed efficiency compared to the ND group, and no significant changes were observed in the 40EEHT treatment groups. Additionally, energy intake and water intake were comparable among the groups.

3.2. Effect of 40EEHT on the weights of organs and adipose tissues in HFD-fed rats

As the results listed in Table 2, the results of kidney, spleen, lung, and heart weights exhibited comparable among the groups. The liver weight of HFD-fed rats was markedly greater than in ND-fed rats (19.66 ± 0.67 vs. 13.73 ± 0.42 g). Additionally, 40EEHT dose-dependently and significantly decreased liver weights in the HFD groups. Our findings indicated that all adipose tissue weights were elevated after HFD feeding. In the HFD + 500 mg/kg 40EEHT group, markedly reduced weights of mesenteric, retroperitoneal, and perirenal adipose tissues were observed. The weights of inguinal and epididymal adipose tissues presented no marked changes among the HFD groups after 40EEHT treatment.

3.3. Effect of 40EEHT on biochemical parameters in serum of HFD-fed rats

As shown in Table 3, serum biochemical parameters indicated markedly elevated levels of triglycerides, ketone bodies, and potassium, along with decreased levels of uric acid and chloride in the HFD group. However, triglyceride (TG), total cholesterol (TC), alanine aminotransferase (ALT),

Table 1. Effect of 40EEHT on physiological parameters in high-fat diet-induced obese rats.

Growth parameters	ND	HFD + 40% ethanol extract of Hsian-tsao (mg/kg rat)			
		0	100	200	500
Initial body weight (g)	219.70 ± 3.10^{a}	224.90 ± 2.53^{a}	221.18 ± 4.27^{a}	218.72 ± 4.33^{a}	215.33 ± 4.60^{a}
Final body weight (g)	440.08 ± 9.43^{d}	549.54 ± 12.73^{a}	537.77 ± 12.68^{ab}	507.36 ± 14.45^{bc}	490.48 ± 10.45^{c}
Weight change (g)	220.38 ± 8.20^{d}	324.64 ± 12.45^{a}	316.59 ± 9.84^{ab}	288.64 ± 13.03^{bc}	275.15 ± 9.78^{c}
Feed intake (g/rat/day)	20.40 ± 0.30^{a}	19.76 ± 0.37^{ab}	19.56 ± 0.37^{ab}	19.28 ± 0.51^{ab}	19.00 ± 0.24^{b}
Feed efficiency (%)	25.41 ± 0.74^{b}	38.24 ± 1.28^{a}	35.98 ± 1.33^{a}	38.01 ± 1.13^{a}	36.68 ± 0.98^{a}
Energy intake (kcal/rat/day)	102.46 ± 1.47^{a}	105.43 ± 2.12^{a}	104.63 ± 1.95^{a}	103.19 ± 2.73^{a}	99.70 ± 1.31^{a}
Water intake (mL/rat/day)	30.58 ± 2.02^{a}	29.89 ± 2.07^{a}	27.43 ± 1.10^{a}	28.95 ± 3.02^{a}	31.08 ± 1.22^{a}

The reported values are the mean ± SEM (n = 10). The mean values with different letters were significantly different ($p < 0.05$). ND, normal diet; HFD, high-fat diet. Weight change (g) = final body weight (g) − initial body weight (g). Feed efficiency (%) = [weight change (g)/total food intake (g)] × 100%.

Table 2. Effect of 40EEHT on the weights of organs and adipose tissues in high-fat diet-induced obese rats.

Organs and tissues weights (g)	ND	HFD + 40% ethanol extract of Hsian-tsao (mg/kg rat)			
		0	100	200	500
Kidney	3.27 ± 0.10^{a}	3.48 ± 0.08^{a}	3.42 ± 0.09^{a}	3.42 ± 0.09^{a}	3.34 ± 0.08^{a}
Liver	13.73 ± 0.42^{d}	19.66 ± 0.67^{a}	17.67 ± 0.50^{b}	16.13 ± 0.56^{c}	14.44 ± 0.44^{d}
Spleen	0.91 ± 0.04^{a}	1.01 ± 0.04^{a}	0.97 ± 0.04^{a}	0.98 ± 0.05^{a}	0.88 ± 0.05^{a}
Lung	1.93 ± 0.09^{a}	2.31 ± 0.18^{a}	1.94 ± 0.03^{a}	2.15 ± 0.08^{a}	2.31 ± 0.16^{a}
Heart	1.39 ± 0.03^{a}	1.43 ± 0.04^{a}	1.48 ± 0.03^{a}	1.46 ± 0.03^{a}	1.40 ± 0.03^{a}
Mesenteric adipose tissue	18.43 ± 0.92^{c}	29.21 ± 2.46^{a}	25.61 ± 2.02^{ab}	23.87 ± 2.13^{abc}	22.51 ± 1.45^{bc}
Retroperitoneal adipose tissue	20.52 ± 1.07^{bc}	27.92 ± 2.75^{a}	26.64 ± 2.60^{ab}	23.90 ± 2.61^{abc}	18.64 ± 2.34^{c}
Inguinal adipose tissue	8.59 ± 1.28^{b}	17.06 ± 2.15^{a}	16.95 ± 2.81^{a}	15.17 ± 1.33^{a}	13.40 ± 1.43^{ab}
Perirenal adipose tissue	24.39 ± 1.79^{c}	40.89 ± 2.76^{a}	37.31 ± 2.14^{ab}	34.66 ± 3.39^{ab}	31.49 ± 2.10^{bc}
Epididymal adipose tissue	17.68 ± 1.10^{b}	29.36 ± 1.68^{a}	29.39 ± 1.75^{a}	26.58 ± 2.11^{a}	24.74 ± 1.14^{a}

The reported values are the mean ± SEM (n = 10). Mean values with different letters were significantly different ($p < 0.05$).

Table 3. Effect of 40EEHT on the serum biochemical parameters in high-fat diet-induced obese rats.

Serum biochemical parameters	ND	HFD + 40% ethanol extract of Hsian-tsao (mg/kg rat)			
		0	100	200	500
Triglyceride (mg/dL)	61.30 ± 5.52^{c}	115.50 ± 14.76^{a}	96.40 ± 13.97^{ab}	71.50 ± 7.36^{bc}	65.60 ± 5.16^{c}
Total cholesterol (mg/dL)	78.80 ± 3.97^{ab}	93.50 ± 4.91^{a}	82.70 ± 6.48^{a}	64.70 ± 5.47^{b}	63.50 ± 4.73^{b}
LDL-cholesterol (mg/dL)	14.40 ± 1.49^{a}	13.20 ± 1.68^{a}	10.80 ± 1.09^{ab}	10.70 ± 1.28^{ab}	8.30 ± 1.18^{b}
Glucose (mg/dL)	217.70 ± 4.11^{a}	224.55 ± 4.86^{a}	223.59 ± 11.51^{a}	221.62 ± 11.58^{a}	222.45 ± 9.53^{a}
AST (U/L)	116.30 ± 12.47^{a}	105.50 ± 7.94^{ab}	89.20 ± 6.54^{b}	86.20 ± 2.94^{b}	83.30 ± 7.21^{b}
ALT (U/L)	50.20 ± 9.75^{ab}	55.80 ± 5.29^{a}	44.10 ± 3.69^{ab}	35.60 ± 2.75^{c}	36.20 ± 3.15^{b}
Uric acid (mg/dL)	6.27 ± 0.37^{a}	4.33 ± 0.32^{b}	5.43 ± 0.26^{a}	5.46 ± 0.36^{a}	5.89 ± 0.38^{a}
Creatinine (mg/dL)	0.75 ± 0.03^{ab}	0.78 ± 0.02^{a}	0.78 ± 0.02^{a}	0.70 ± 0.02^{b}	0.72 ± 0.01^{ab}
Ketone body (mmol/L)	5.85 ± 0.15^{d}	10.99 ± 0.69^{a}	8.65 ± 0.21^{b}	7.60 ± 0.24^{c}	4.35 ± 0.22^{e}
Na (mmol/L)	151.50 ± 0.50^{a}	151.30 ± 1.05^{a}	152.10 ± 1.00^{a}	147.00 ± 0.33^{b}	147.60 ± 0.27^{b}
K (mmol/L)	6.78 ± 0.27^{b}	8.18 ± 0.75^{a}	5.85 ± 0.24^{b}	7.02 ± 0.34^{ab}	6.82 ± 0.32^{b}
Cl (mmol/L)	98.40 ± 0.67^{a}	96.40 ± 0.53^{b}	98.00 ± 0.47^{ab}	97.60 ± 0.45^{ab}	97.50 ± 0.52^{ab}

The reported values are the mean ± SEM (n = 10). The mean values with different letters were significantly different ($p < 0.05$).

and sodium levels were significantly decreased in the HFD groups after treatment with 200 and 500 mg/kg 40EEHT. A significantly lower LDL-C level was observed in the HFD + 500 mg/kg 40EEHT group. Uric acid levels were significantly increased following the 40EEHT intervention, while creatinine levels were markedly reduced in the HFD + 200 mg/kg 40EEHT group. In HFD-fed rats, 40EEHT treatment demonstrated a dose-dependent reduction in ketone body levels. A significant decline in potassium levels was found in the HFD + 100 mg/kg and 500 mg/kg 40EEHT groups. AST and chloride levels remained comparable in the HFD groups after 40EEHT treatment, and glucose levels showed no significant differences among the groups.

3.4. Effect of 40EEHT on the fecal and hepatic total lipids in HFD-fed rats

Table 4 demonstrated significantly elevated levels of hepatic cholesterol, triglycerides, and total lipids in HFD-fed rats, which were markedly reduced following treatment with 200 and 500 mg/kg 40EEHT. Additionally, fecal triglyceride, cholesterol, and total lipid levels were significantly increased in the HFD-fed rats. The excretion of cholesterol,

Table 4. Effect of 40EEHT on the total lipid, triglyceride, and cholesterol of liver and feces in high-fat diet-induced obese rats.

Contents (mg/g)	ND	HFD + 40% ethanol extract of Hsian-tsao (mg/kg rat)			
		0	100	200	500
Hepatic triglyceride	14.10 ± 0.80^{c}	38.90 ± 1.71^{a}	36.79 ± 1.54^{ab}	32.15 ± 3.24^{b}	32.73 ± 1.82^{b}
Hepatic cholesterol	20.13 ± 0.41^{b}	28.63 ± 2.63^{a}	27.25 ± 1.13^{ab}	25.31 ± 1.41^{b}	25.27 ± 0.86^{b}
Hepatic total lipid	42.30 ± 1.49^{c}	82.31 ± 7.16^{a}	71.79 ± 2.47^{ab}	69.20 ± 3.84^{b}	66.81 ± 2.46^{b}
Fecal triglyceride	13.13 ± 1.03^{d}	28.35 ± 1.28^{c}	37.91 ± 5.34^{b}	60.97 ± 1.10^{a}	62.23 ± 2.09^{a}
Fecal cholesterol	8.68 ± 0.28^{e}	14.94 ± 1.03^{d}	27.82 ± 3.40^{c}	45.22 ± 0.98^{b}	51.46 ± 2.28^{a}
Fecal total lipid	71.93 ± 1.04^{d}	136.66 ± 9.10^{c}	176.05 ± 8.94^{b}	184.03 ± 9.72^{a}	186.34 ± 13.27^{a}

The reported values are the mean ± SEM (n = 10). The mean values with different letters were significantly different ($p < 0.05$).

triglycerides, and total lipids in feces was found to increase with higher doses of 40EEHT treatment.

3.5. Effect of 40EEHT on the histology of perirenal adipose and hepatic tissues in HFD-fed rats

Compared to ND rats, fat deposition in hepatic tissue and the enlarged size of perirenal adipocytes were significantly increased in HFD-fed rats. Reduced hepatic fat accumulation was observed with increasing concentrations of 40EEHT (Fig. 1A upper panel). Furthermore, treatment with 200 and 500 mg/kg 40EEHT significantly reduced perirenal adipocyte hypertrophy in HFD-induced obese rats (Fig. 1A lower panel and 1B).

3.6. Effects of 40EEHT on the serum and hepatic antioxidant capacity in HFD-fed rats

Significantly increased MDA levels and decreased TEAC levels were observed in both the liver and serum after HFD feeding. The results showed no significant difference in serum TEAC levels after 40EEHT treatment. However, serum MDA levels were significantly reduced after treatment with 500 mg/kg 40EEHT. In the liver of HFD-fed rats, TEAC levels were significantly elevated, and MDA levels were markedly reduced following 40EEHT treatment. The levels of GSSG, GSH, GRd, GST, GPx, and catalase were markedly decreased after HFD feeding. However, treatment with 100 and 500 mg/kg 40EEHT significantly increased GSH and GSSG contents in the HFD rats. Additionally, 40EEHT treatment markedly induced GST and GPx levels in obese rats. GRd and catalase levels in HFD-fed rats did not show significant changes following the 40EEHT intervention (Table 5).

3.7. Effects of 40EEHT on the lipid metabolism of perirenal adipose tissue in HFD-fed rats

The results indicated that *SIRT1* levels were markedly elevated in a dose-dependent manner with 40EEHT treatment (Fig. 2A), and the expression levels of *ACC* and *FAS* were significantly decreased following 40EEHT treatment (Fig. 2B and 2C). *FATP1* and *CD36* levels were also markedly reduced by 40EEHT treatment in obese rats (Fig. 2D and 2E). Moreover, 40EEHT significantly increased the levels of *AMPK*, *CPT-1*, and *ACO* (Fig. 2F, G, and 2H). Additionally, 40EEHT induced *ATGL* and *HSL* levels in a dose-dependent manner (Fig. 2I and 2J). Meanwhile,

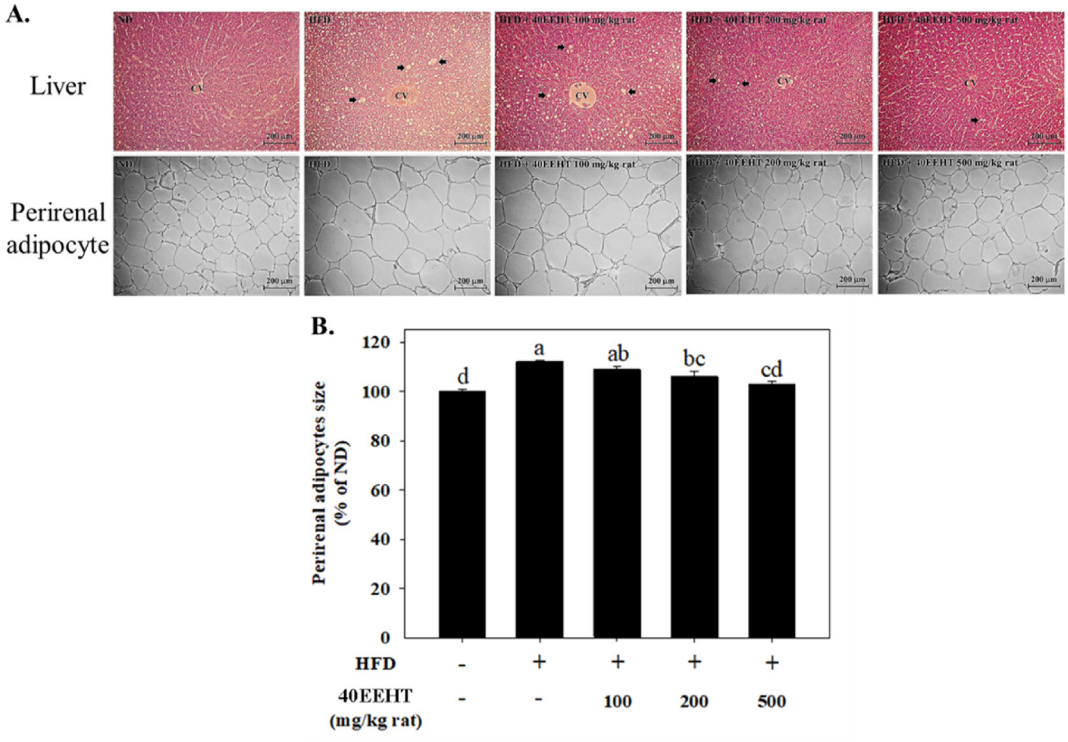

Fig. 1. ***Effect of 40EEHT on liver and perirenal adipocytes in obese rats induced by the high-fat diet.*** *(A) Liver and perirenal adipose tissues were stained with hematoxylin and eosin (H&E). Original magnification: 200× . (B) Percentage (%) is expressed as normal diet (ND) at 100%. The reported values are the mean ± SEM (n = 3). The mean values with different letters were significantly different (p < 0.05).*

Table 5. Effect of 40EEHT on lipid metabolism in high-fat diet-induced obese rats.

Oxidative stress and antioxidant enzymes	ND	HFD + 40% ethanol extract of Hsian-tsao (mg/kg rat)			
		0	100	200	500
Serum TEAC (μmol/mL serum)	20.76 ± 1.06^{a}	14.65 ± 2.11^{b}	15.91 ± 0.63^{b}	15.02 ± 1.06^{b}	14.33 ± 0.25^{b}
Serum MDA (nmol/mL serum)	1.37 ± 0.17^{b}	2.05 ± 0.20^{a}	2.02 ± 0.10^{a}	1.99 ± 0.20^{a}	1.16 ± 0.13^{b}
Hepatic TEAC (μmol/mg protein)	0.18 ± 0.01^{a}	0.05 ± 0.01^{c}	0.09 ± 0.01^{b}	0.10 ± 0.02^{b}	0.10 ± 0.02^{b}
Hepatic MDA (nmol/mg protein)	0.10 ± 0.00^{b}	0.12 ± 0.01^{a}	0.05 ± 0.00^{d}	0.08 ± 0.01^{c}	0.10 ± 0.01^{bc}
Hepatic GSSG (nmol/mg protein)	13.17 ± 0.46^{a}	9.67 ± 0.38^{b}	7.66 ± 0.22^{cd}	8.94 ± 0.84^{bc}	6.61 ± 0.58^{d}
Hepatic GSH (nmol/mg protein)	32.19 ± 1.03^{a}	23.78 ± 0.94^{b}	19.14 ± 0.62^{c}	22.95 ± 2.06^{b}	17.06 ± 1.48^{c}
Hepatic GST (nmol/min/mg protein)	0.14 ± 0.00^{b}	0.13 ± 0.00^{c}	0.15 ± 0.00^{b}	0.16 ± 0.00^{a}	0.14 ± 0.00^{b}
Hepatic GRd (nmol/min/mg protein)	21.22 ± 1.03^{a}	15.21 ± 0.56^{b}	15.46 ± 0.36^{b}	17.41 ± 1.29^{b}	17.54 ± 0.89^{b}
Hepatic GPx (nmol/min/mg protein)	5.88 ± 1.57^{b}	2.25 ± 0.35^{c}	5.68 ± 0.70^{b}	9.63 ± 1.14^{a}	8.54 ± 0.46^{ab}
Hepatic catalase (unit/min/mg protein)	6.48 ± 0.32^{a}	4.71 ± 0.20^{bc}	4.02 ± 0.11^{c}	4.85 ± 0.37^{b}	4.87 ± 0.22^{b}

The reported values are the mean ± SEM (n = 10). The mean values with different letters were significantly different ($p < 0.05$). Trolox equivalent antioxidant capacity, TEAC; Malondialdehyde, MDA; Glutathione, GSH; Glutathione disulfide, GSSG; Glutathione S-transferase, GST; Glutathione reductase, GRd; Glutathione peroxidase, GPx.

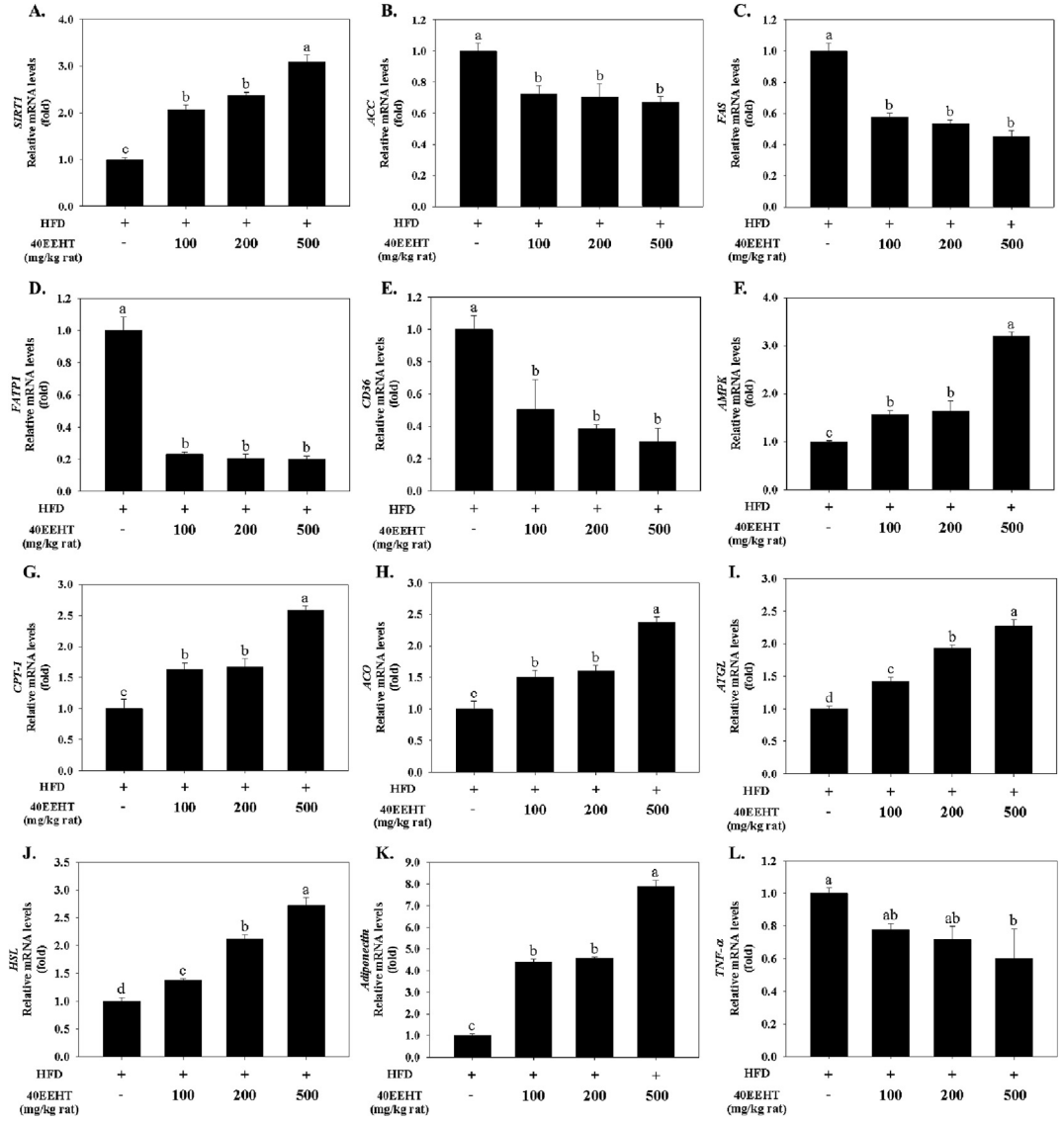

Fig. 2. ***Effect of the 40% ethanol extract of Hsian-tsao on the gene expressions of fatty acid metabolism in the perirenal adipose tissue of obese rats induced by a high-fat diet.*** *The reported values are the mean ± SEM (n = 3). The mean values with different letters were significantly different ($p < 0.05$). The values of SIRT1, ACC, FAS, FATP1, CD36, AMPK, CPT-1, ACO, ATGL, HSL, adiponectin, and TNF-α mRNA were normalized to the value of β-actin. SIRT1, sirtuin 1; ACC, acetyl-CoA carboxylase; FAS, fatty acid synthase; FATP1, fatty acid transport protein 1; CD36, differentiation 36; AMPK, AMP-activated protein kinase; CPT-1, carnitine palmitoyltransferase 1; ACO, acyl-CoA oxidase; ATGL, adipose triacylglycerol lipase; HSL, hormone sensitive lipase; TNF-α, tumor necrosis factor-α.*

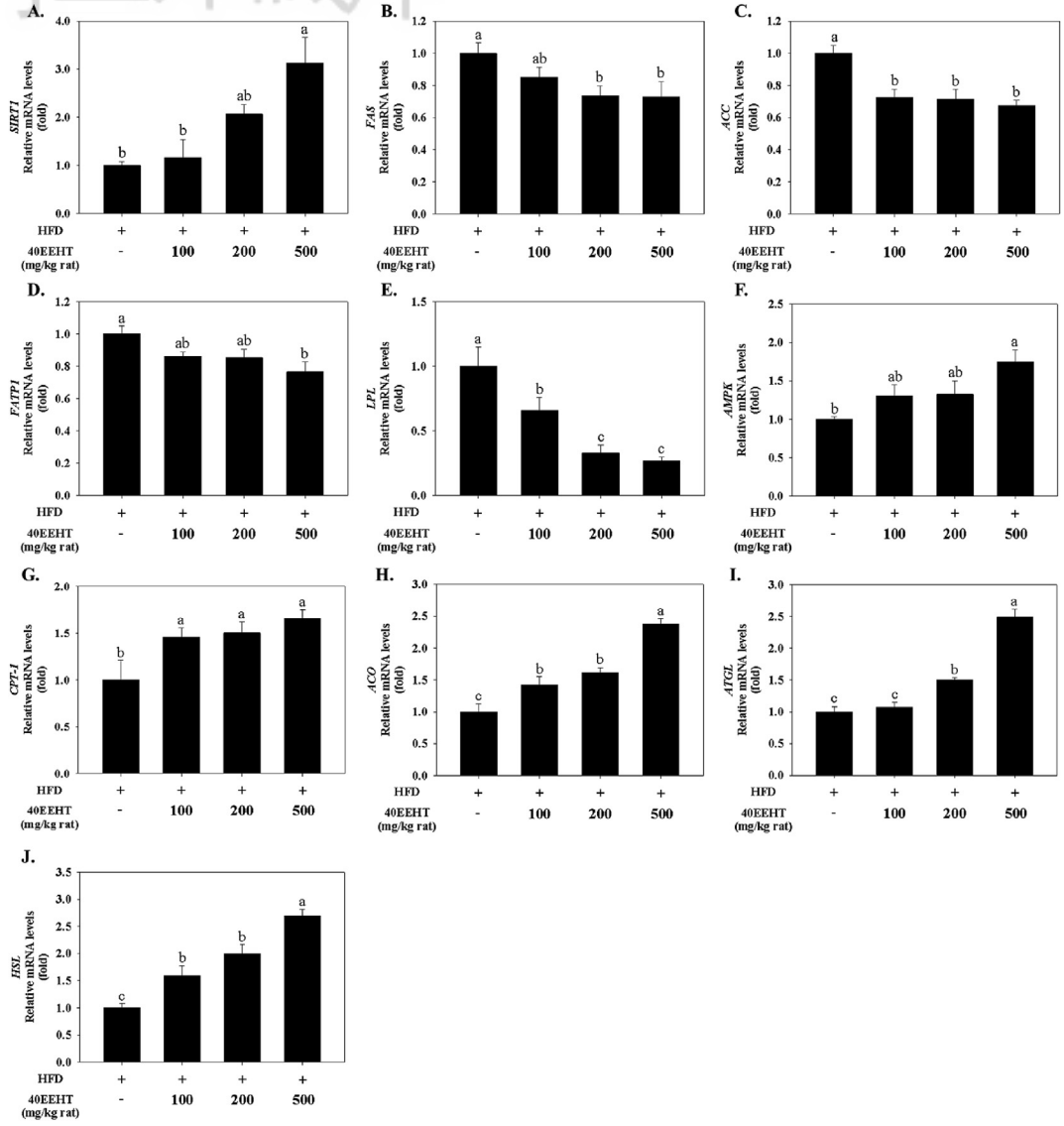

Fig. 3. ***Effect of the 40% ethanol extract of Hsian-tsao on the gene expressions of fatty acid metabolism in the liver of obese rats.*** *The reported values are the mean ± SEM ($n = 3$). The mean values with different letters were significantly different ($p < 0.05$). The values of SIRT1, ACC, FAS, FATP1, LPL, AMPK, CPT-1, ACO, ATGL, and HSL mRNA were normalized to the value of β-actin. SIRT1, sirtuin 1; ACC, acetyl-CoA carboxylase; FAS, fatty acid synthase; FATP1, fatty acid transport protein 1; LPL, lipoprotein lipase; AMPK, AMP-activated protein kinase; CPT-1, carnitine palmitoyltransferase 1; ACO, acyl-CoA oxidase; ATGL, adipose triacylglycerol lipase; HSL, hormone sensitive lipase.*

HFD-inhibited adiponectin levels (Fig. 2K) were significantly elevated with an increased dose of 40EEHT, and *TNF-α* levels (Fig. 2L) were markedly reduced in the HFD + 500 mg/kg 40EEHT group.

3.8. Effect of 40EEHT on lipid metabolism of hepatic tissue in HFD-fed rats

In liver tissue, *SIRT1* levels were markedly elevated in the HFD + 500 mg/kg 40EEHT group (Fig. 3A). *FAS* levels were significantly decreased in the HFD + 200 mg/kg and 500 mg/kg 40EEHT groups (Fig. 3B), while *ACC* levels were significantly reduced after 40EEHT treatment (Fig. 3C) ($p < 0.05$). *FATP1* levels were markedly reduced in the HFD + 500 mg/kg 40EEHT group (Fig. 3D), and *LPL* levels were reduced after 40EEHT treatment (Fig. 3E). In the HFD + 500 mg/kg 40EEHT group, a significantly increased *AMPK* level was observed (Fig. 3F) ($p < 0.05$), 40EEHT significantly increased hepatic *CPT-1* and *ACO* levels in the HFD-fed groups (Fig. 3G and H). Moreover, the hepatic *ATGL* level (Fig. 3I) showed a marked increase in the HFD + 200 mg/kg and 500 mg/kg 40EEHT groups, and 40EEHT dose-dependently increased *HSL* levels in HFD-induced rats (Fig. 3J) ($p < 0.05$).

4. Discussion

Excessive dietary fat is a core factor contributing to obesity-related syndromes, including arteriosclerosis, hypertension, hyperlipidemia, respiratory complications, type 2 diabetes, osteoarthritis, and cancer [37]. HFD-induced animal obesity models are commonly used to elucidate the progression of metabolic syndromes, which may help in developing effective strategies for prevention and improvement [1,38,39]. Numerous studies have shown that high-fat diets induce obesity in mice and rats [40,41], and such diets alter energy metabolism and induce lipid accumulation [42,43]. In our study, after 8 weeks of feeding with a high-fat diet (32% fat/g diet) and 40EEHT, we found that 40EEHT markedly reduced body weight gain in rats without affecting feed intake, water intake, energy intake, or feed efficiency (Table 1). In HFD-fed rats, the extract of *Clinacanthus nutans*, which contains phenolic acids with strong antioxidant capacities, significantly decreased body weight gain induced by HFD [44]. Similarly, Irfan et al. (2022) indicated that elevated body weight and obesity-related metabolic syndrome were significantly reversed by treatment with *Moringa oleifera* leaf extracts for 30 days [45].

The liver is a fundamental metabolic organ in the body, and a high-calorie diet is associated with a high incidence of hepatic diseases, including cirrhosis, liver cancer, and nonalcoholic fatty liver disease [46–48]. Adipose tissue plays a critical role in fat storage, cytokine secretion, and energy homeostasis, and a long-term high-fat diet leads to increased adipose tissue weight in rats [49,50]. In our study, 40EEHT significantly reduced the increased weights of the liver and total body fat induced by HFD feeding (Table 2). Morphological analysis of perirenal adipose and hepatic tissues in obese rats revealed lipid droplet accumulation in the liver and enlarged perirenal adipocytes, which were reversed by 40EEHT treatment (Fig. 1). Lee et al. (2014) reported that *Codonopsis lanceolata* extracts significantly reduced body fat mass and weight gain in HFD-fed mice [51]. Similarly, Amor et al. (2019) demonstrated that body weight gain and subcutaneous fat weight were markedly decreased by aging black garlic extract in obese rats [52]. Previous animal and clinical studies have indicated that treatments with phytochemicals such as curcumin, rutin, epigallocatechin gallate, gallic acid, and o-coumaric acid improve HFD-induced dyslipidemia [53–56]. Our findings indicate that 40EEHT markedly reduced the levels of triglycerides (TG), total cholesterol (TC), LDL-C, ALT, ketone bodies, sodium ions, and potassium ions in serum (Table 3). Noh and Yoon (2022) also demonstrated that the ethanol extract of mulberry ameliorates dyslipidemia and hepatic steatosis by decreasing hepatic triglycerides, serum LDL-C, cholesterol, and the TC/HDL-C ratio [57].

In vivo studies have revealed that the progression of obesity is correlated with reduced antioxidant activities and increased oxidative stress in blood, tissues, and organs [23,58,59]. Reactive oxygen species (ROS) play a crucial role in the pathogenesis of hyperlipidemia [60]. ROS are primarily generated via lipid accumulation and β-oxidation in fatty liver [61]. Antioxidant enzyme systems, such as GST, GPx, and GRd, can neutralize ROS, reduce oxidative stress, and eliminate free radicals [62]. Furthermore, obesity is characterized by fatty acid peroxidation, with malondialdehyde (MDA) serving as a primary biomarker of fatty acid oxidation [58,63,64]. In the antioxidant activity analysis, 40EEHT significantly ameliorated MDA levels in serum, as well as MDA, TEAC, GPx, and GST levels in the liver of HFD-fed rats (Table 5). The water extract of *Clerodendron glandulosum* Coleb, rich in phenolic compounds, has been shown to increase the excretion of triglycerides, cholesterol, bile acids, and total lipids in rat feces [65]. A recent study demonstrated that flavonoids from *Lycium barbarum* leaves can reverse body weight gain, improve serum and hepatic lipid profiles, reduce oxidative stress, increase fecal lipid excretion, and alleviate glucose tolerance [66]. In our previous study, black garlic reduced body weight, liver weight, epididymal fat, peritoneal fat, hepatic lipid profiles, and serum triglycerides. Additionally, black garlic elevated hepatic GRd, GPx, GSH, and TEAC levels while reducing GSSG, thereby suppressing oxidative stress in HFD-fed SD rats [67]. Our results suggest that the HFD group supplemented with 40EEHT exhibited markedly increased fecal lipid profiles (cholesterol, triglycerides, and total lipids), which were reversed by 40EEHT treatment (Table 4). A high-fat diet induces malabsorption and metabolic alterations in the gut, leading to elevated excretion of lipids, triglycerides, and cholesterol in feces [68]. These alterations, such as intestinal saturation, altered gut microbiota, and lipase inhibition, contribute to incomplete absorption of high levels of dietary fat, resulting in excess fat being excreted in the feces [69–71]. Previous studies have shown that the anti-obesity effects of *Platycodi radix* water extract and peanut shell ethanol extract might suppress pancreatic lipase activity, leading to delayed lipid absorption in the intestine and increased lipid excretion in feces [72,73]. Another report indicated that the *C. glandulosum* Coleb extract, containing phenolic

compounds, promotes the excretion of fecal bile acids, triglycerides, cholesterol, and total lipids in high-fat diet-fed rats [74]. Yeh et al. (2009) found that caffeic acid markedly inhibited cholesterol absorption and elevated fecal cholesterol excretion in rats [75]. Ginger extract, rich in phenolic compounds, significantly reduced hepatic lipid profiles and increased fecal lipid profiles through miR-21/132 suppression and AMPK signaling activation [76]. Yu et al. (2021) demonstrated that berberine down-regulated CD36 and SCD1 in the gut, leading to stimulated fat excretion in feces [77]. Similarly, in our investigation, 40EEHT triggered AMPK activation and CD36 inhibition.

The regulation of lipid metabolism in hepatic and perirenal adipose tissues of HFD-fed obese rats was explored to elucidate the efficiency of the anti-obesity properties of 40EEHT *in vivo* (Figs. 2 and 3). A crucial function of SIRT1 is to regulate the expression of genes involved in energy metabolism, including those related to fatty acid synthesis (*FAS* and *ACC*) [78–80]. Our results showed that different doses of 40EEHT treatment significantly enhanced *SIRT1* levels and inhibited lipogenesis in HFD-induced rats (Figs. 2 and 3). Vanillic acid, caffeic acid, *p*-coumaric acid, and chlorogenic acid were identified in the 80% methanol extract of *Sasa borealis bamboo* stem, which significantly inhibited hepatic *FAS*, *ACC*, *SREBP-1c*, and *PPAR-γ* in HFD-fed obese rats [81]. BinMowyna et al. (2022) demonstrated that resveratrol enhanced hepatic *PPARα* levels and suppressed liver *SREBP1* and *SREBP2* levels by inhibiting miR-34a and inducing *SIRT1*, which significantly improved insulin sensitivity and fatty liver disease in HFD-induced rats [82].

aP2, FATP1, CD36, and LPL play critical roles in lipid transport and metabolism [83]. LPL releases triglycerides from lipoproteins in VLDL and chylomicrons, directing them into the liver for metabolism or storage in adipose tissue [84]. Additionally, aP2, FATP1, and CD36 enhance fatty acid uptake, contributing to obesity [85,86]. Our findings suggest that 40EEHT significantly reduces the expression of genes associated with lipid transport and storage in the hepatic and perirenal adipose tissues of rats (Figs. 2 and 3). In a recent investigation, the methanol extract of Hsian-tsao was found to significantly reduce fat accumulation by inhibiting the PPARγ and C/EBPα signaling pathway in 3T3-L1 adipocytes [19].

AMPK is an essential regulator of fatty acid metabolism *in vivo*, controlling *ACC* and *FAS* in fatty acid synthesis, as well as β-oxidation processes involving *ACO* and *CPT-1* [87–90]. According to our findings, 40EEHT markedly induced β-oxidation in the liver and perirenal fat of HFD-fed rats (Figs. 2 and 3). Guo et al. (2016) demonstrated that phenolic compounds from the Chenpi n-butane extract significantly increased *AMPK* levels in the perirenal adipose tissue of HFD-fed C57BL/6J obese mice [91]. Furthermore, berbamine significantly reversed weight gain and lipid accumulation in the liver by reducing *FAS* and *SCD1* levels and inhibiting *ACC* levels through the SIRT1/LKB1/AMPK axis in NAFLD rats [92]. Miao sour soup markedly reduced FAS, ACC, and SREBP-1c levels through the regulation of AMPK activation, while alleviating fat accumulation in obese rats [93].

ATGL and HSL play vital roles in lipolysis [94]. Our results show that 40EEHT significantly enhanced lipolysis in the perirenal fat and liver of HFD-induced rats (Figs. 2 and 3). Choi et al. (2016) indicated that green coffee bean extracts, which contain caffeic acid and chlorogenic acid, markedly induced the levels of *CPT-1*, *PPAR-α*, *HSL*, and *ATGL* while suppressing the levels of *SREBP-1c* and *PPAR-γ* in perirenal adipose tissue. Additionally, in hepatic tissue, these extracts elevated *AMPK*, *PPAR-α*, and *CPT-1* levels and reduced *FAS*, *SREBP-1c*, and *PPAR-γ* levels in HFD-induced mice [95]. Wu et al. (2021) demonstrated that lipid accumulation and body weight gain were reversed by lemon-fermented products, which inhibited *C/EBPα*, *PPARγ*, and *SREBP-1c* levels and induced *HSL* and *ATGL* levels via the AMPK pathway in epididymal adipose and hepatic tissues in HCD-induced rats [96].

Adipose tissue plays a vital role in the endocrine system by producing hormones such as adiponectin and TNF-α. Obesity increases the concentration of TNF-α, which is correlated with chronic inflammation and insulin resistance [97]. Conversely, adiponectin has anti-inflammatory effects and improves metabolic syndrome [98,99]. Our findings suggest that 40EEHT significantly decreased *TNF-α* levels and increased adiponectin levels. Alam et al. (2016) indicated that caffeic acid, chlorogenic acid, and p-coumaric acid promote the secretion of adiponectin and reduce *TNF-α* levels in adipose tissue, thereby improving obesity and related complications [100]. Sant'Ana et al. (2022) suggested that macauba pulp oil increased adiponectin and inhibited *TNF-α*, *NF-κB*, *SREBP-1c*, and *PPAR-γ* in adipose tissue while reducing the expression of hepatic *CPT-1α* and *SREBP-1c*, leading to the prevention of adipogenesis in obese C57BL/6 mice [101].

In conclusion, 40EEHT reduces body weight gain, total body fat, serum lipid profiles, and hepatic lipid profiles by modulating fatty acid metabolism in

hepatic and adipose tissues. Our report suggests that the ethanol extract of Hsian-tsao has beneficial effects in suppressing HFD-induced obesity in rats.

Funding

This research work was supported by Chung Shan Medical University (the grant NCHU-CSMU 10609), Taichung, Taiwan.

Conflict of interest

The authors declare that no conflicts of interest exist.

References

[1] Hariri N, Thibault L. High-fat diet-induced obesity in animal models. Nutr Res Rev 2010;23:270–99.
[2] Withrow D, Alter DA. The economic burden of obesity worldwide: a systematic review of the direct costs of obesity. Obes Rev 2011;12:131–41.
[3] Hodson L, Gunn PJ. The regulation of hepatic fatty acid synthesis and partitioning: the effect of nutritional state. Nat Rev Endocrinol 2019;15:689–700.
[4] Redinger RN. Fat storage and the biology of energy expenditure. Transl Res 2009;154:52–60.
[5] Hammarstedt A, Gogg S, Hedjazifar S, Nerstedt A, Smith U. Impaired adipogenesis and dysfunctional adipose tissue in human hypertrophic obesity. Physiol Rev 2018;98:1911–41.
[6] Stubbs RJ, Harbron CG, Murgatroyd PR, Prentice AM. Covert manipulation of dietary fat and energy density: effect on substrate flux and food intake in men eating ad libitum. Am J Clin Nutr 1995;62:316–29.
[7] Huang J, Wang Y, Xie Z, Zhou Y, Zhang Y, Wan X. The anti-obesity effects of green tea in human intervention and basic molecular studies. Eur J Clin Nutr 2014;68:1075–87.
[8] Jiao W, Mi S, Sang Y, Jin Q, Chitrakar B, Wang X, et al. Integrated network pharmacology and cellular assay for the investigation of an anti-obesity effect of 6-shogaol. Food Chem 2022;374:131755.
[9] Polat S, Trif M, Rusu A, Šimat V, Čagalj M, Alak G, et al. Recent advances in industrial applications of seaweeds. Crit Rev Food Sci Nutr 2023;63:4979–5008.
[10] Huang Y, Cai P, Su X, Zheng M, Chi W, Lin S, et al. Hsian-Tsao (Mesona chinensis Benth.) extract improves the thermal tolerance of Drosophila melanogaster. Front Nutr 2022;9:819319.
[11] Jhang J-J, Ong J-W, Lu C-C, Hsu C-L, Lin J-H, Liao J-W, et al. Hypouricemic effects of Mesona procumbens Hemsl. through modulating xanthine oxidase activity in vitro and in vivo. Food Funct 2016;7:4239–46.
[12] Yeh YH, Liang CY, Chen ML, Tsai FM, Lin YY, Lee MC, et al. Apoptotic effects of hsian-tsao (Mesona procumbens Hemsley) on hepatic stellate cells mediated by reactive oxygen species and ERK, JNK, and caspase-3 pathways. Food Sci Nutr 2019;7:1891–8.
[13] Yen G-C, Yeh C-T, Chen Y-J. Protective effect of Mesona procumbens against tert-butyl hydroperoxide-induced acute hepatic damage in rats. J Agric Food Chem 2004;52:4121–7.
[14] Huang GJ, Liao JC, Chiu CS, Huang SS, Lin TH, Deng JS. Anti-inflammatory activities of aqueous extract of Mesona procumbens in experimental mice. J Sci Food Agric 2012;92:1186–93.
[15] Huang H-C, Chuang S-H, Wu Y-C, Chao P-M. Hypolipidaemic function of Hsian-tsao tea (Mesona procumbens Hemsl.): working mechanisms and active components. J Funct Foods 2016;26:217–27.
[16] Niu G, You G, Zhou X, Fan H, Liu X. Physicochemical properties and in vitro hypoglycemic activities of hsian-tsao polysaccharide fractions by gradient ethanol precipitation method. Int J Biol Macromol 2023;231:123274.
[17] Yen G-C, Duh P-D, Hung Y-L. Contributions of major components to the antimutagenic effect of Hsian-Tsao (Mesona procumbens Hemsl.). J Agric Food Chem 2001;49:5000–4.
[18] Yen G-C, Hung C-Y. Effects of alkaline and heat treatment on antioxidative activity and total phenolics of extracts from Hsian-tsao (Mesona procumbens Hemsl.). Food Res Int 2000;33:487–92.
[19] Huang H-T, Liaw C-C, Chiou C-T, Lee K-T, Kuo Y-H, Mesonosides AH. Primeverose derivatives from Mesona procumbens suppress adipogenesis by downregulating PPARγ and C/EBPα in 3T3-L1 cells. J Food Drug Anal 2021;29:448.
[20] Fan S-L, Lin J-A, Chen S-Y, Lin J-H, Lin H-T, Chen Y-Y, et al. Effects of Hsian-tsao (Mesona procumbens Hemsl.) extracts and its polysaccharides on the promotion of wound healing under diabetes-like conditions. Food Funct 2021;12:119–32.
[21] Castro JP, Grune T, Speckmann B. The two faces of reactive oxygen species (ROS) in adipocyte function and dysfunction. Biol Chem 2016;397:709–24.
[22] Liu G-S, Chan EC, Higuchi M, Dusting GJ, Jiang F. Redox mechanisms in regulation of adipocyte differentiation: beyond a general stress response. Cells 2012;1:976–93.
[23] Pérez-Torres I, Castrejón-Téllez V, Soto ME, Rubio-Ruiz ME, Manzano-Pech L, Guarner-Lans V. Oxidative stress, plant natural antioxidants, and obesity. Int J Mol Sci 2021;22:1786.
[24] Zielinska-Blizniewska H, Sitarek P, Merecz-Sadowska A, Malinowska K, Zajdel K, Jablonska M, et al. Plant extracts and reactive oxygen species as two counteracting agents with anti-and pro-obesity properties. Int J Mol Sci 2019;20:4556.
[25] Hung C-Y, Yen G-C. Antioxidant activity of phenolic compounds isolated from Mesona procumbens Hemsl. J Agric Food Chem 2002;50:2993–7.
[26] Xu J, Ge J, He X, Sheng Y, Zheng S, Zhang C, et al. Caffeic acid reduces body weight by regulating gut microbiota in diet-induced-obese mice. J Funct Foods 2020;74:104061.
[27] Nathu H, Mbuyama KR, Adarkwah-Yiadom M, Serem JC, Ibrahim MA, Duodu KG, et al. Antioxidant properties and inhibition of lipid formation in 3T3-L1 adipocytes of in vitro digested mageu, a commercial sample. J Food Biochem 2021;45:e13929.
[28] Akram A, Jamshed A, Anwaar M, Rasheed HMF, Haider SI, Aslam N, et al. Evaluation of Caralluma edulis for its potential against obesity, atherosclerosis and hypertension. Dose Response 2023;21:15593258231152112.
[29] Fischer AH, Jacobson KA, Rose J, Zeller R. Hematoxylin and eosin staining of tissue and cell sections. Cold Spring Harb Protoc 2008;2008. pdb. prot4986.
[30] Tzang B-S, Yang S-F, Fu S-G, Yang H-C, Sun H-L, Chen Y-C. Effects of dietary flaxseed oil on cholesterol metabolism of hamsters. Food Chem 2009;114:1450–5.
[31] Arts MJ, Haenen GR, Voss H-P, Bast A. Antioxidant capacity of reaction products limits the applicability of the Trolox Equivalent Antioxidant Capacity (TEAC) assay. Food Chem Toxicol 2004;42:45–9.
[32] Bird R, Draper H. Comparative studies on different methods of malonaldehyde determination. Methods Enzymol 1984:299–305.
[33] Lawrence RA, Burk RF. Glutathione peroxidase activity in selenium-deficient rat liver. Biochem Biophys Res Commun 1976;71:952–8.
[34] Bellomo G, Mirabelli F, DiMonte D, Richelmi P, Thor H, Orrenius C, et al. Formation and reduction of glutathione-protein mixed disulfides during oxidative stress: a study with isolated hepatocytes and menadione (2-methyl-1, 4-naphthoquinone). Biochem Pharmacol 1987;36:1313–20.

[35] Shangari N, O'Brien PJ. Catalase activity assays. Curr Protoc Toxicol 2006;27(7.. 1–7):16.

[36] Livak KJ, Schmittgen TD. Analysis of relative gene expression data using real-time quantitative PCR and the 2−ΔΔCT method. Methods 2001;25:402–8.

[37] Kopelman PG. Obesity as a medical problem. Nature 2000; 404:635–43.

[38] Buettner R, Schölmerich J, Bollheimer LC. High-fat diets: modeling the metabolic disorders of human obesity in rodents. Obesity 2007;15:798–808.

[39] Panchal SK, Brown L. Rodent models for metabolic syndrome research. BioMed Res Int 2011;2011.

[40] Park YS, Yoon Y, Ahn HS. Platycodon grandiflorum extract represses up-regulated adipocyte fatty acid binding protein triggered by a high fat feeding in obese rats. World J Gastroenterol 2007;13:3493.

[41] Tsuda T, Horio F, Uchida K, Aoki H, Osawa T. Dietary cyanidin 3-O-β-D-glucoside-rich purple corn color prevents obesity and ameliorates hyperglycemia in mice. J Nutr 2003; 133:2125–30.

[42] Iossa S, Lionetti L, Mollica MP, Crescenzo R, Botta M, Barletta A, et al. Effect of high-fat feeding on metabolic efficiency and mitochondrial oxidative capacity in adult rats. Br J Nutr 2003;90:953–60.

[43] Pagliassotti MJ, Gayles EC, Hill JO. Fat and energy balance. Ann N Y Acad Sci 1997;827:431–48.

[44] Sarega N, Imam MU, Ooi D-J, Chan KW, Md Esa N, Zawawi N, et al. Phenolic rich extract from Clinacanthus nutans attenuates hyperlipidemia-associated oxidative stress in rats. Oxid Med Cell Longev 2016;2016.

[45] Irfan M, Munir H, Ismail H. Moringa oleifera gum based silver and zinc oxide nanoparticles: green synthesis, characterization and their antibacterial potential against MRSA. Biomater Res 2021;25:17.

[46] Kakimoto PA, Kowaltowski AJ. Effects of high fat diets on rodent liver bioenergetics and oxidative imbalance. Redox Biol 2016;8:216–25.

[47] Schaffer JE. Lipotoxicity: when tissues overeat. Curr Opin Lipidol 2003;14:281–7.

[48] Zhang S, Zheng L, Dong D, Xu L, Yin L, Qi Y, et al. Effects of flavonoids from Rosa laevigata Michx fruit against high-fat diet-induced non-alcoholic fatty liver disease in rats. Food Chem 2013;141:2108–16.

[49] Ghibaudi L, Cook J, Farley C, Van Heek M, Hwa JJ. Fat intake affects adiposity, comorbidity factors, and energy metabolism of Sprague-Dawley rats. Obes Res 2002;10: 956–63.

[50] Rosen ED, Spiegelman BM. Adipocytes as regulators of energy balance and glucose homeostasis. Nature 2006;444: 847–53.

[51] Lee JS, Kim K-J, Kim Y-H, Kim D-B, Shin G-H, Cho J-H, et al. Codonopsis lanceolata extract prevents diet-induced obesity in C57BL/6 mice. Nutrients 2014;6:4663–77.

[52] Amor S, González-Hedström D, Martín-Carro B, Inarejos-García AM, Almodóvar P, Prodanov M, et al. Beneficial effects of an aged black garlic extract in the metabolic and vascular alterations induced by a high fat/sucrose diet in male rats. Nutrients 2019;11:153.

[53] Hsu C-L, Wu C-H, Huang S-L, Yen G-C. Phenolic compounds rutin and o-coumaric acid ameliorate obesity induced by high-fat diet in rats. J Agric Food Chem 2009;57: 425–31.

[54] Hsu C-L, Yen G-C. Effect of gallic acid on high fat diet-induced dyslipidaemia, hepatosteatosis and oxidative stress in rats. Br J Nutr 2007;98:727–35.

[55] Mohammadi A, Sahebkar A, Iranshahi M, Amini M, Khojasteh R, Ghayour-Mobarhan M, et al. Effects of supplementation with curcuminoids on dyslipidemia in obese patients: a randomized crossover trial. Phytother Res 2013; 27:374–9.

[56] Ramesh E, Elanchezhian R, Sakthivel M, Jayakumar T, Senthil Kumar R, Geraldine P, et al. Epigallocatechin gallate improves serum lipid profile and erythrocyte and cardiac tissue antioxidant parameters in Wistar rats fed an atherogenic diet. Fundam Clin Pharmacol 2008;22:275–84.

[57] Noh D-j, Yoon G-A. Mulberry (Morus alba L.) ethanol extract attenuates lipid metabolic disturbance and adipokine imbalance in high-fat fed rats. Nutr Res Prac 2022;16: 716–28.

[58] Olusi S. Obesity is an independent risk factor for plasma lipid peroxidation and depletion of erythrocyte cytoprotectic enzymes in humans. Int J Obes 2002;26:1159–64.

[59] Ozata M, Mergen M, Oktenli C, Aydin A, Sanisoglu SY, Bolu E, et al. Increased oxidative stress and hypozincemia in male obesity. Clin Biochem 2002;35:627–31.

[60] Young IS, McEneny J. Lipoprotein oxidation and atherosclerosis. Biochem Soc Trans 2001;29:358–62.

[61] Pettinelli P, Obregón A, Videla L. Molecular mechanisms of steatosis in nonalcoholic fatty liver disease. Nutr Hosp 2011; 26:441–50.

[62] Husain K, Mejia J, Lalla J, Kazim S. Dose response of alcohol-induced changes in BP, nitric oxide and antioxidants in rat plasma. Pharmacol Res 2005;51:337–43.

[63] Nielsen F, Mikkelsen BB, Nielsen JB, Andersen HR, Grandjean P. Plasma malondialdehyde as biomarker for oxidative stress: reference interval and effects of life-style factors. Clin Chem 1997;43:1209–14.

[64] Yesilbursa D, Serdar Z, Serdar A, Sarac M, Coskun S, Jale C. Lipid peroxides in obese patients and effects of weight loss with orlistat on lipid peroxides levels. Int J Obes 2005;29:142–5.

[65] Jadeja RN, Thounaojam MC, Dandekar DS, Devkar RV, Ramachandran A. Clerodendron glandulosum. Coleb extract ameliorates high fat diet/fatty acid induced lipotoxicity in experimental models of non-alcoholic steatohepatitis. Food Chem Toxicol 2010;48:3424–31.

[66] Liao J, Guo J, Niu Y, Fang T, Wang F, Fan Y. Flavonoids from Lycium barbarum leaves attenuate obesity through modulating glycolipid levels, oxidative stress, and gut bacterial composition in high-fat diet-fed mice. Front Nutr 2022;9:972794.

[67] Chang W-T, Shiau D, Cheng M, Tseng C, Chen C, Wu M, et al. Black garlic ameliorates obesity induced by a high-fat diet in rats. J Food Nutr Res 2017;5:736–41.

[68] Araújo JR, Tomas J, Brenner C, Sansonetti PJ. Impact of high-fat diet on the intestinal microbiota and small intestinal physiology before and after the onset of obesity. Biochimie 2017;141:97–106.

[69] Aron-Wisnewsky J, Warmbrunn MV, Nieuwdorp M, Clément K. Metabolism and metabolic disorders and the microbiome: the intestinal microbiota associated with obesity, lipid metabolism, and metabolic health—pathophysiology and therapeutic strategies. Gastroenterology 2021;160:573–99.

[70] Murakami Y, Tanabe S, Suzuki T. High-fat diet-induced intestinal hyperpermeability is associated with increased bile acids in the large intestine of mice. J Food Sci 2016;81: H216–22.

[71] Park H, Bae SH, Park Y, Choi HS, Suh HJ. Lipase-mediated lipid removal from propolis extract and its antiradical and antimicrobial activity. J Sci Food Agric 2015;95:1697–705.

[72] Han L-K, Kimura Y, Okuda H, Xu B-J, Zheng Y-n. Platycodi radix affects lipid metabolism in mice with high fat diet–induced obesity. J Nutr 2000;130:2760–4.

[73] Moreno DA, Ilic N, Poulev A, Raskin I. Effects of Arachis hypogaea nutshell extract on lipid metabolic enzymes and obesity parameters. Life Sci 2006;78:2797–803.

[74] Jadeja R, Thounaojam M, Devkar R, Ramachandran A. Clerodendron glandulosum Coleb., Verbenaceae, ameliorates high fat diet-induced alteration in lipid and cholesterol metabolism in rats. Rev Bras Farmacogn 2010;20: 117–23.

[75] Yeh Y-H, Lee Y-T, Hsieh H-S, Hwang D-F. Dietary caffeic acid, ferulic acid and coumaric acid supplements on cholesterol metabolism and antioxidant activity in rats. J Food Drug Anal 2009;17:4.

[76] Kim S, Lee MS, Jung S, Son HY, Park S, Kang B, et al. Ginger extract ameliorates obesity and inflammation via regulating MicroRNA-21/132 expression and AMPK activation in white adipose tissue. Nutrients 2018;10.
[77] Yu M, Alimujiang M, Hu L, Liu F, Bao Y, Yin J. Berberine alleviates lipid metabolism disorders via inhibition of mitochondrial complex I in gut and liver. Int J Biol Sci 2021; 17:1693−707.
[78] Boutant M, Cantó C. SIRT1 metabolic actions: integrating recent advances from mouse models. Mol Metabol 2014;3: 5−18.
[79] Rahman S, Islam R. Mammalian Sirt1: insights on its biological functions. Cell Commun Signal 2011;9:1−8.
[80] Wilentz RE, Witters LA, Pizer ES. Lipogenic enzymes fatty acid synthase and acetyl-coenzyme A carboxylase are coexpressed with sterol regulatory element binding protein and Ki-67 in fetal tissues. Pediatr Dev Pathol 2000; 3:525−31.
[81] Song Y, Lee S-J, Jang S-H, Ha JH, Song YM, Ko Y-G, et al. Sasa borealis stem extract attenuates hepatic steatosis in high-fat diet-induced obese rats. Nutrients 2014;6:2179−95.
[82] BinMowyna MN, AlFaris NA, Al-Sanea EA, AlTamimi JZ, Aldayel TS. Resveratrol attenuates against high-fat-diet-promoted non-alcoholic fatty liver disease in rats mainly by targeting the miR-34a/SIRT1 axis. Arch Physiol Biochem 2022:1−16.
[83] Wu C, Chu E, Lam C, Cheng A, Lee C, Wong V, et al. PPARγ is essential for protection against nonalcoholic steatohepatitis. Gene Ther 2010;17:790−8.
[84] Wang H, Eckel RH. Lipoprotein lipase: from gene to obesity. Am J Physiol Endocrinol Metab 2009;297:E271−88.
[85] Choi H, Kim S-J, Park S-S, Chang C, Kim E. TR4 activates FATP1 gene expression to promote lipid accumulation in 3T3-L1 adipocytes. FEBS Lett 2011;585:2763−7.
[86] Wu Q, Ortegon AM, Tsang B, Doege H, Feingold KR, Stahl A. FATP1 is an insulin-sensitive fatty acid transporter involved in diet-induced obesity. Mol Cell Biol 2006;26: 3455−67.
[87] Alberdi G, Rodríguez VM, Macarulla MT, Miranda J, Churruca I, Portillo MP. Hepatic lipid metabolic pathways modified by resveratrol in rats fed an obesogenic diet. Nutrition 2013;29:562−7.
[88] Duplus E, Forest C. Is there a single mechanism for fatty acid regulation of gene transcription? Biochem Pharmacol 2002;64:893−901.
[89] Hardie D, Pan D. Regulation of fatty acid synthesis and oxidation by the AMP-activated protein kinase. Biochem Soc Trans 2002;30:1064−70.
[90] Kondo T, Kishi M, Fushimi T, Kaga T. Acetic acid upregulates the expression of genes for fatty acid oxidation enzymes in liver to suppress body fat accumulation. J Agric Food Chem 2009;57:5982−6.
[91] Guo J, Tao H, Cao Y, Ho C-T, Jin S, Huang Q. Prevention of obesity and type 2 diabetes with aged citrus peel (Chenpi) extract. J Agric Food Chem 2016;64:2053−61.
[92] Sharma A, Anand SK, Singh N, Dwarkanath A, Dwivedi UN, Kakkar P. Berbamine induced activation of the SIRT1/LKB1/AMPK signaling axis attenuates the development of hepatic steatosis in high-fat diet-induced NAFLD rats. Food Funct 2021;12:892−909.
[93] Yang H, Xie J, Wang N, Zhou Q, Lu Y, Qu Z, et al. Effects of Miao sour soup on hyperlipidemia in high-fat diet-induced obese rats via the AMPK signaling pathway. Food Sci Nutr 2021;9:4266−77.
[94] Gaidhu MP, Anthony NM, Patel P, Hawke TJ, Ceddia RB. Dysregulation of lipolysis and lipid metabolism in visceral and subcutaneous adipocytes by high-fat diet: role of ATGL, HSL, and AMPK. Am J Physiol Cell Physiol 2010;298: C961−71.
[95] Choi B-K, Park S-B, Lee D-R, Lee HJ, Jin Y-Y, Yang SH, et al. Green coffee bean extract improves obesity by decreasing body fat in high-fat diet-induced obese mice. Asian Pac J Tropical Med 2016;9:635−43.
[96] Wu C-C, Huang Y-W, Hou C-Y, Chen Y-T, Dong C-D, Chen C-W, et al. The anti-obesity effects of lemon fermented products in 3T3-L1 preadipocytes and in a rat model with high-calorie diet-induced obesity. Nutrients 2021;13:2809.
[97] Makki K, Froguel P, Wolowczuk I. Adipose tissue in obesity-related inflammation and insulin resistance: cells, cytokines, and chemokines. Int Sch Res Notices 2013;2013.
[98] Hector J, Schwarzloh B, Goehring J, Strate T, Hess U, Deuretzbacher G, et al. TNF-α alters visfatin and adiponectin levels in human fat. Horm Metab Res 2007;39:250−5.
[99] Lihn A, Pedersen SB, Richelsen B. Adiponectin: action, regulation and association to insulin sensitivity. Obes Rev 2005;6:13−21.
[100] Alam MA, Subhan N, Hossain H, Hossain M, Reza HM, Rahman MM, et al. Hydroxycinnamic acid derivatives: a potential class of natural compounds for the management of lipid metabolism and obesity. Nutr Metab 2016;13:1−13.
[101] Sant'Ana CT, Agrizzi Verediano T, Grancieri M, Toledo RCL, Tako E, Costa NMB, et al. Macauba (Acrocomia aculeata) pulp oil prevents adipogenesis, inflammation and oxidative stress in mice fed a high-fat diet. Nutrients 2023;15:1252.